

# Shear behavior of CoCrFeNiCuTi<sub>x</sub> high-entropy alloys based on molecular dynamics simulations

Yitao Liu<sup>1</sup>, Dongrong Xin<sup>1\*</sup>

<sup>1</sup>College of Civil Engineering, Fujian University of Technology, Fuzhou, China

\*Corresponding Author. Email: drxin@fjut.edu.cn

**Abstract.** This study uses molecular dynamics simulations to systematically explore the effects of Ti content, temperature, and shear strain rate on the shear deformation behavior of CoCrFeNiCuTi<sub>x</sub> High-Entropy Alloys (HEAs). The results show that, at the same temperature and shear strain rate, the shear modulus increases with the increase in Ti content, while the shear strength remains unaffected. For the equiatomic CoCrFeNiCuTi high-entropy alloy, both the shear modulus and shear strength decrease linearly as the temperature rises. However, as the shear strain rate increases, the shear modulus remains mostly unchanged, but the shear strength shows a significant increase.

**Keywords:** CoCrFeNiCuTi high-entropy alloy, molecular dynamics simulation, shear deformation, Ti content, shear strain rate

## 1. Introduction

Metals, as one of the most important materials in the development of human civilization, play a significant role in mechanical manufacturing, electronics, electrical appliances, aerospace, and other fields. Traditional alloys usually enhance their physicochemical properties by adding small amounts of other elements to a single metal. However, the strengthening effects of such alloys have gradually reached a bottleneck. With the development of technology and engineering applications in the 21st century, traditional alloys have increasingly struggled to meet extreme demands such as radiation resistance, corrosion resistance, high strength, and high wear resistance.

These technological bottlenecks have led to a revolution in alloy material design concepts. In the early 21st century, Taiwanese scholar Yeh [1] proposed the concept of High-Entropy Alloys (HEAs), which are composed of four or more elements and have high configurational entropy.

High-entropy alloys' multi-principal element characteristic not only exhibits superior mechanical properties, such as high strength, high wear resistance, and fatigue resistance, compared to traditional metals, but their unique lattice distortion and material disorder offer more possibilities for controlling their performance. However, the preparation of high-entropy alloys and the complex interactions brought by their multiple elements have made it a significant challenge to study their microscopic physicochemical mechanisms through traditional physical testing methods.

In this context, Molecular Dynamics (MD) simulations, as a simulation tool, have provided a unique research paradigm for investigating the properties of high-entropy alloys. The essence of MD is to simulate various atomic changes by solving the atomic motion equations through finite difference methods. For extreme conditions (such as radiation environments, high-temperature and high-pressure environments, etc.) or complex materials, MD simulations can significantly reduce the cost of material composition optimization and field testing, providing relatively reasonable theoretical support for the early-stage development and performance prediction of new materials.

In recent years, many scholars at home and abroad have conducted in-depth research on the process, phase transformation mechanisms, and mechanical properties of high-entropy alloys:

Meiske et al. [2] investigated the effect of Deep Cryogenic Treatment Time (DCT) on the microstructure and tribological properties of Al<sub>0.5</sub>CoCrFeNb<sub>0.5</sub>Ni high-entropy alloys. Their results show that deep cryogenic treatment did not induce the formation of new phases, but significantly reduced the content of the BCC phase and altered the distribution of grain sizes (first increasing, then decreasing, and finally increasing again). Furthermore, the combined effect of grain refinement and solid solution strengthening led to a significant increase in microhardness. They also pointed out the evolution of wear mechanisms with DCT time: over short durations, wear was primarily caused by oxidation, adhesion, and abrasive wear, while over longer durations, it

shifted to oxidation and fatigue wear. This provides important theoretical support for the optimization and performance regulation of deep cryogenic treatment for AlCoCrFeNi high-entropy alloys.

He et al. [3] studied the effect of Ti content on the microstructure and mechanical properties of  $\text{Co}_{39.2}\text{Ni}_{39.2}\text{Al}_{21.6-x}\text{Ti}_x$  dual-phase high-entropy alloys. Their experiments highlighted the role of Ti in regulating phase composition, precipitate characteristics, and deformation mechanisms. Raman et al. [4] investigated the high-temperature deformation behavior of equimolar CrMoNbTiW refractory high-entropy alloys prepared by mechanical alloying and spark plasma sintering at temperatures ranging from 1000 to 1350°C and under different strain rates. Their experiments revealed that the CrMoNbTiW high-entropy alloy mainly consists of a BCC phase, accompanied by a multi-phase microstructure with TiC and  $\text{Cr}_2\text{Nb}$  secondary phases. Qiu et al. [5] explored the effect of laser energy density on the properties of AlCoCrFeNi<sub>2.1</sub> dual-phase eutectic high-entropy alloy coatings, elucidating the evolution of the ratio between the FCC and BCC phases under energy density control and the correlation with mechanical properties. This provided a theoretical basis for the process optimization and toughening design of high-entropy alloy coatings.

Cui's team [6] used Dual-Glow Plasma Surface Alloying Technology (DGPSA) to prepare a CoCrFeNiMn high-entropy alloy hard coating on the surface of Invar alloy. They analyzed the microstructure of the coating using X-Ray Diffraction (XRD), Scanning Electron Microscopy (SEM), and Energy Dispersive Spectroscopy (EDS). Yang et al. [7] systematically studied the effect of Al content on the radiation resistance of Al<sub>x</sub>CrMoNbZr high-entropy alloy coatings. They found that the addition of aluminum enhanced radiation stability by strengthening lattice distortion effects and inhibiting defect migration. This provided key experimental evidence for the material design of radiation-resistant high-entropy alloy coatings.

Wang et al. [8] summarized the preparation methods of high-entropy alloys and recent research progress, focusing on the process principles and application cases of laser cladding, mechanical alloying, and vacuum melting. They explained the mechanisms of grain refinement and thermal stability improvement through various preparation methods.

As a newly emerging multi-element alloy material, CoCrFeNiCuTi high-entropy alloys have not been fully studied in terms of their mechanical properties. Therefore, the authors have conducted a preliminary study on the shear deformation of CoCrFeNiCuTi high-entropy alloys using Molecular Dynamics (MD) simulations. This provides guidance and reference for further understanding the complex mechanical properties and constitutive relationships of CoCrFeNiCuTi high-entropy alloys.

## 2. Model construction

### 2.1. Modeling of CoCrFeNiCuTix high-entropy alloys

Li and Xiang's team [9] determined through XRD that the phase structure of CoCrFeNiCuTi high-entropy alloys is composed of a single FCC phase. Teams from Miao, Liu [10], and Shi [11] also identified FCC as the predominant crystal structure of CoCrFeNiCuTi alloys through X-ray diffraction. This study models the CoCrFeNiCuTi high-entropy alloy using the open-source software LAMMPS, with CoCrFeNiCu alloy as the base (FCC crystal structure), and Ti atoms are randomly inserted to form the CoCrFeNiCuTix high-entropy alloy model.

The model has dimensions of 7.12 nm × 7.12 nm × 7.12 nm, containing a total of 32,000 atoms. To eliminate the effects of boundary conditions and size, periodic boundary conditions are applied. The schematic diagram of the model is shown in Figure 1.

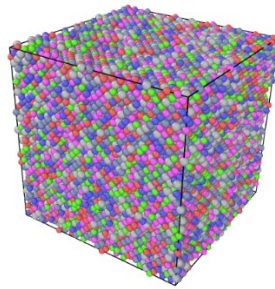


**Figure 1.** Model ( $x, y, z = 7.12 \text{ nm} \times 7.12 \text{ nm} \times 7.12 \text{ nm}$ )

### 2.2. Potential function

For the CoCrFeNiCuTix high-entropy alloy, since no dedicated potential function has been developed for it, a mixed potential approach is adopted in this study. Ti atoms use the eam/fs potential proposed by Mendev et al. [12], and the CoCrFeNiCu alloy base uses the eam/alloy potential developed by Farkas and Caro [13]. The interactions between Ti atoms and other atoms in the alloy are set using the lj/cut potential [14-17].

### 2.3. Energy minimization and relaxation

The system is first minimized using the conjugate gradient method, with energy tolerance ( $1.0e-8$ ) and force tolerance ( $1.0e-10$ ).

Next, relaxation is performed under the Isothermal-Isobaric Ensemble (NPT) to bring the system to equilibrium. The relaxation parameters are set to a temperature of 300 K, pressure of 0 Pa, and a total simulation time of 10 ps (with a time step of 0.001 ps, totaling 10,000 steps). The relaxation process is shown in Figure 2.

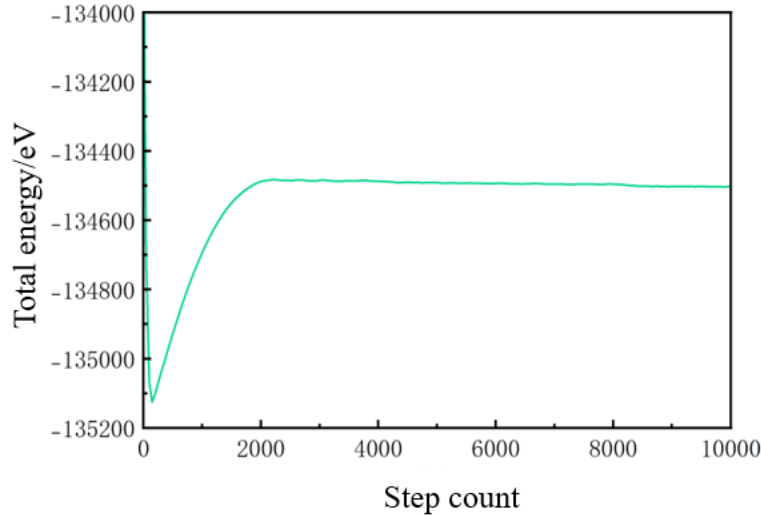


**Figure 2.** Relaxation total energy curve

### 3. Influence and analysis of Ti content on shear deformation of CoCrFeNiCuTi high-entropy alloy

To investigate the changes in shear properties of CoCrFeNiCuTi high-entropy alloy at different titanium contents, this study constructed an alloy system model with a composition of  $Fe:Ni:Cr:Co:Cu:Ti = 1:1:1:1:1:x$ , where  $x$  was set to 0.25, 0.50, 0.75, and 1.00 (corresponding to titanium contents of 4.8%, 9.1%, 13.0%, and 16.7%, respectively). All simulation processes were conducted under an Isothermal-Isobaric Ensemble (NPT), with a shear strain rate of  $0.01 \text{ ps}^{-1}$  and a pressure of 0 Pa.

Figures 3, 4, and 5 show the shear stress-strain curve, shear modulus vs. Ti content curve, and shear strength vs. Ti content curve, respectively.

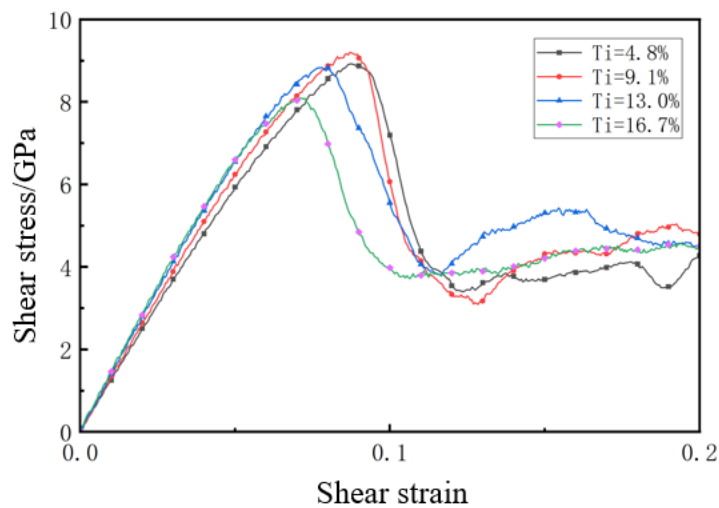


**Figure 3.** Stress-strain curves of CoCrFeNiCuTi high-entropy alloys with different Ti contents

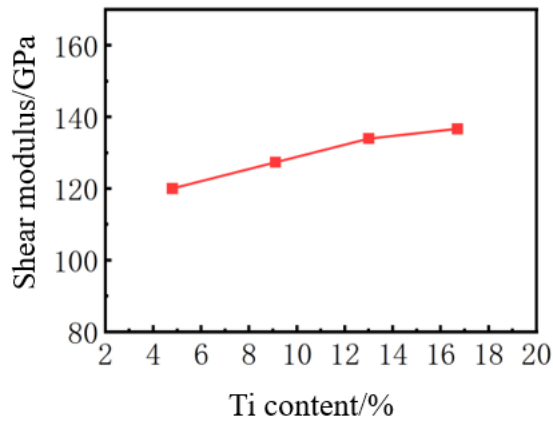


**Figure 4.** Shear modulus- Ti content curve

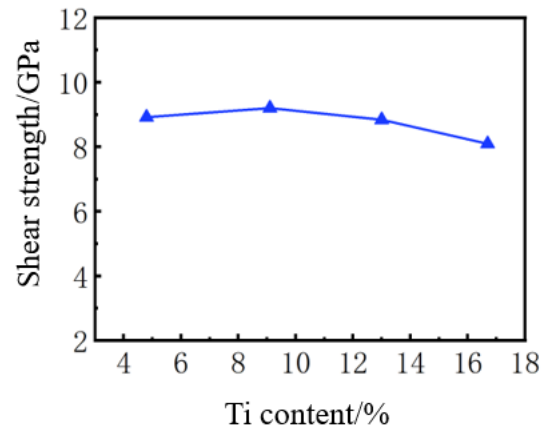


**Figure 5.** Shear strength- Ti content curve

From Figures 3, 4, and 5, it can be observed that as the Ti content increases, the shear modulus of CoCrFeNiCuTi high-entropy alloy also gradually increases. The shear modulus increased from 119.98 GPa at  $Ti = 4.8\%$  to 136.61 GPa at  $Ti = 16.7\%$ , an increase of 13.86%. However, the shear strength showed no significant change. This might be because the addition of Ti enhanced the atomic bonding energy, but the alloy still maintained a single FCC phase, causing no significant change in the resistance to dislocation motion (e.g., lattice resistance, solid solution atom pinning effect).

The quantitative statistical results are shown in Table 1.

**Table 1.** Shear modulus and shear strength of high entropy alloy with different Ti contents

Ti Content (%)	4.8%	9.1%	13.0%	16.7%
Shear Modulus /GPa	119.98	127.35	133.94	136.61
Shear Strength /GPa	8.92	9.20	8.84	8.09

#### 4. Influence and analysis of temperature on shear deformation of CoCrFeNiCuTi high-entropy alloy

To explore the changes in shear properties of CoCrFeNiCuTi high-entropy alloy at different temperatures, this study used an equimolar high-entropy alloy model (1:1:1:1:1, with Ti content of 16.7%) and constructed a temperature gradient simulation system ranging from 100K to 900K (with temperature points every 200K). All shear simulations were conducted under an Isothermal-Isobaric Ensemble (NPT), with a shear strain rate of  $0.01 \text{ ps}^{-1}$  and a pressure of 0 Pa.

Figures 6, 7, and 8 show the shear stress-strain curve, shear modulus vs. temperature curve, and shear strength vs. temperature curve, respectively.

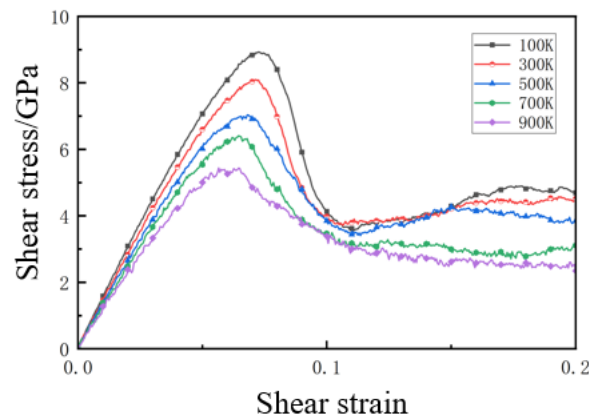


**Figure 6.** Stress-strain curves of CoCrFeNiCuTi high-entropy alloy at different temperatures

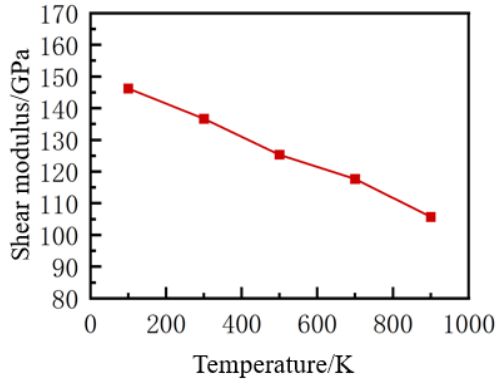


**Figure 7.** Shear modulus-temp curve

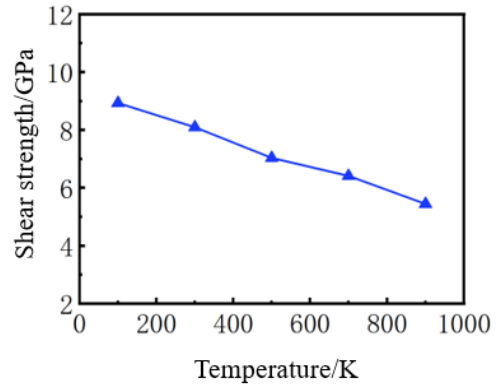


**Figure 8.** Shear strength-temp curve

From Figures 6, 7, and 8, it can be observed that as the system temperature increases, the shear modulus of CoCrFeNiCuTi high-entropy alloy gradually decreases. The shear modulus decreased from 146.16 GPa at 100K to 105.67 GPa at 900K, a reduction of 38.32%.

The shear strength also showed an approximately linear decrease as the system temperature increased, from 8.93 GPa at 100K to 5.44 GPa at 900K, a reduction of 64.15%. This is likely due to the increased atomic thermal motion with temperature, which weakens atomic bonding. Additionally, at high temperatures, the activation energy for dislocation motion decreases, making dislocation slip more easily, resulting in the observed decline in shear modulus and shear strength.

The quantitative statistical results are shown in Table 2.

**Table 2.** Shear modulus and shear strength of high entropy alloy at different temperatures

Temperature/K	100	300	500	700	900
Shear Modulus/GPa	146.16	136.61	125.30	117.66	105.67
Shear Strength/GPa	8.93	8.09	7.03	6.41	5.44

### 5. Influence and analysis of shear strain rate on shear deformation of CoCrFeNiCuTi high-entropy alloy

To investigate the changes in shear properties of CoCrFeNiCuTi high-entropy alloy at different shear strain rates, this study used the same equimolar high-entropy alloy model (1:1:1:1:1, with Ti content of 16.7%) and simulated different shear strain rates.

Four shear strain rates were used: 0.01 ps<sup>-1</sup>, 0.025 ps<sup>-1</sup>, 0.075 ps<sup>-1</sup>, and 0.1 ps<sup>-1</sup>. All shear simulations were conducted under an Isothermal-Isobaric Ensemble (NPT), with a system temperature of 300K and a pressure of 0 Pa.

Figures 9, 10, and 11 show the shear stress-strain curve, shear modulus vs. shear strain rate curve, and shear strength vs. shear strain rate curve, respectively.

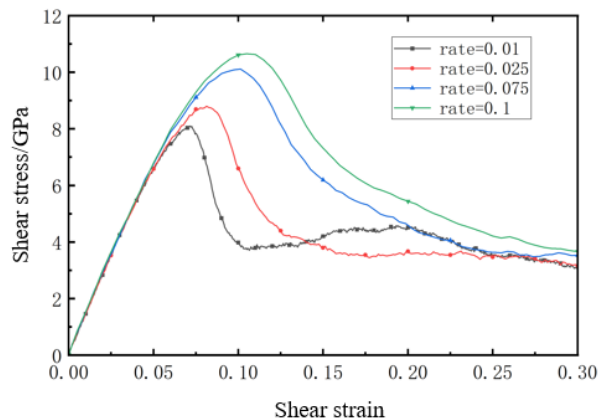


**Figure 9.** Stress-strain curves of CoCrFeNiCuTi high entropy alloy at different shear strain rates

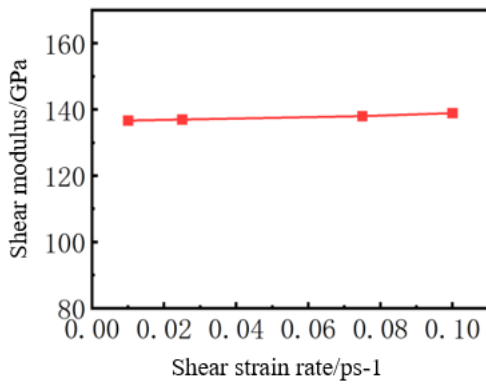


**Figure 10.** Shear modulus-shear strain rate curve

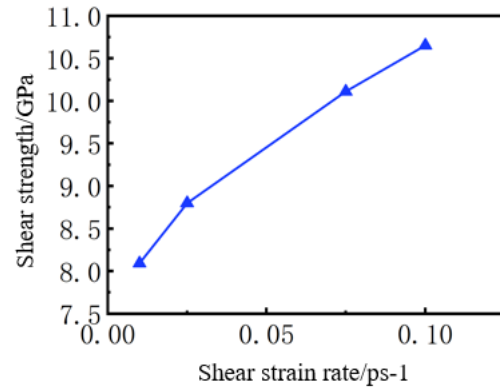


**Figure 11.** Shear strength-shear strain rate curve

From Figures 9, 10, and 11, it can be seen that as the shear strain rate increases, the shear modulus of CoCrFeNiCuTi high-entropy alloy remains nearly constant. This is likely because the shear modulus is primarily determined by the atomic bonding strength and crystal structure at the microscopic level, and its response to strain rate variations is not sensitive in elastic deformation.

However, the shear strength increases with the increase in shear strain rate, rising from 8.09 GPa at 0.01 ps<sup>-1</sup> to 10.65 GPa at 0.1 ps<sup>-1</sup>, an increase of approximately 31.64%. This phenomenon could be caused by dynamic interactions between some atoms and moving dislocations at higher strain rates, leading to a "drag effect" that hinders dislocation slip. Additionally, higher shear strain rates might lead to the formation of nanoscale twins, which enhances shear strength.

The quantitative statistical results are shown in Table 3.

**Table 3.** Shear modulus and shear strength of high entropy alloy at different shear strain rates

Shear Strain Rate/ps <sup>-1</sup>	0.01	0.025	0.075	0.1
Shear Modulus/GPa	136.61	136.96	137.95	138.87
Shear Strength/GPa	8.09	8.80	10.11	10.65

## 6. Conclusion

In this study, the Molecular Dynamics (MD) method was used to systematically investigate the effects of different titanium contents, temperatures, and shear strain rates on the shear deformation of CoCrFeNiCuTi high-entropy alloy. By establishing multiple comparative models, the study primarily focused on exploring the changes in shear modulus and shear strength and the possible mechanisms behind these changes. The main research results are as follows:

1) Under constant temperature conditions (300K), as the titanium content increased from 4.8% to 16.7%, the shear modulus of CoCrFeNiCuTi high-entropy alloy increased from 119.98 GPa to 136.61 GPa, with an increase of about 13.86%. However, the shear strength did not show significant changes within this range of titanium content. This phenomenon could be attributed to the fact that, although the addition of titanium increased atomic bonding energy and thus improved the shear modulus, the CoCrFeNiCuTi high-entropy alloy still maintained a single Face-Centered Cubic (FCC) structure within the experimental variable range. As a result, the resistance to dislocation motion (e.g., lattice resistance and solid solution atom pinning effect) did not change fundamentally.

2) The mechanical properties of CoCrFeNiCuTi high-entropy alloy (with 16.7% titanium content) showed a significant temperature dependence. When the system temperature increased from 100K to 900K, the shear modulus decreased from 146.16 GPa to 105.67 GPa, a reduction of 38.32%. Meanwhile, the shear strength decreased linearly from 8.93 GPa to 5.44 GPa, a reduction of 64.15%. The mechanism behind this could be that the increased temperature enhanced atomic thermal motion, which weakened atomic bonding. Additionally, the activation energy for dislocation motion decreased at higher temperatures, making dislocation slip more easily.

3) For CoCrFeNiCuTi high-entropy alloy (with 16.7% titanium content), the shear modulus remained relatively stable in the shear strain rate range from 0.01 ps<sup>-1</sup> to 0.1 ps<sup>-1</sup>. This phenomenon is likely due to the fact that the shear modulus, as one of the basic material properties, is primarily determined by atomic bonding strength and crystal structure. Therefore, its correlation with strain rate is low during elastic deformation. However, the shear strength exhibited a noticeable rate-strengthening effect. As the shear strain rate increased from 0.01 ps<sup>-1</sup>, where the shear strength was 8.09 GPa, to 0.1 ps<sup>-1</sup>, where the shear strength was 10.65 GPa, the maximum increase in shear strength reached 31.64%. This could be attributed to the dynamic interaction between some atoms and moving dislocations at higher shear strain rates, forming a "drag effect" that hinders dislocation slip. Additionally, higher shear strain rates might lead to the formation of nanoscale twins, which enhance shear strength.

Through molecular dynamics simulations, this study preliminarily explored the mechanical behavior of CoCrFeNiCuTi high-entropy alloy during shear deformation. However, due to the limited experimental conditions and the inherent limitations of molecular simulation (e.g., theoretical modeling cannot truly reflect the actual material manufacturing process and the crystal defect characteristics it brings), this research only provides a preliminary reference for the study of the mechanical properties of CoCrFeNiCuTi high-entropy alloys. Further validation of atomic potential functions for describing novel high-entropy alloys is still needed. It is anticipated that future research, combined with traditional experiments, will establish a more reasonable and comprehensive theoretical framework for the processing and engineering applications of CoCrFeNiCuTi high-entropy alloys.

## References

- [1] Yeh, J. W., Chen, S. K., Lin, S. J., Gan, J. Y., Chin, T. S., Shun, T. T., Tsau, C. H., & Chang, S. Y. (2004). Nanostructured high-entropy alloys with multiple principal elements: Novel alloy design concepts and outcomes. *Advanced Engineering Materials*, 6(5), 299-303.
- [2] Mei, S., Yan, L., & Cai, Z. (2025). Effect of cryogenic treatment time on the microstructure and tribological properties of Al<sub>0.5</sub>CoCrFeNb<sub>0.5</sub>Ni high-entropy alloys. *China Surface Engineering*, 1-16.
- [3] He, Y. X., Liu, H. X., Li, M. Y., Liu, X. D., & Li, J. S. (2024). Effect of Ti content on the microstructure and mechanical properties of Co<sub>39.2</sub>Ni<sub>39.2</sub>Al<sub>21.6-x</sub>Ti<sub>x</sub> dual-phase high-entropy alloys. *Materials Development and Applications*, 39(05), 55-62.
- [4] Raman, L., Anupam, A., Karthick, G., Berndt, C. C., Ang, A. S. M., Murty, S. V. S. N., Fabijanic, D., Murty, B. S., & Kottada, R. S. (2025). High temperature deformation behavior and microstructural evolution of an ultrafine-grained and multiphase CrMoNbTiW refractory high entropy alloy. *Acta Materialia*, 289, 120841.
- [5] Qiu, H., Dong, Z., Feng, L. T., Lin, G. P., Wu, L. H., Le, Y. S., Yan, X. C., & Liu, M. (2025). Study on the effect of laser energy density on the wear and mechanical properties of FCC+BCC dual-phase eutectic high-entropy alloys. *Materials Research and Applications*, 19(01), 155-163.
- [6] Cui, K. J., Wang, J. G., Wang, H. F., Xing, X. G., Xiao, G. S., & Jia, Y. W. (2025). Preparation, microstructure, and mechanical properties of Mo and CoCrFeNiMn high-entropy alloy hard coatings. *Journal of High Pressure Physics*, 1-15.
- [7] Yang, J., Li, H., & Li, H. (2025). Effects of irradiation on the microstructure and mechanical properties of AlxCrMoNbZr high-entropy alloy coatings. *Materials Review*, 1-13.
- [8] Wang, Y., Li, A., & Wei, S. (2021). Research status of preparation methods for high-entropy alloys. *Information Record Materials*, 22(05), 14-17.
- [9] Li, Y. (2018). Study on the microstructure and properties of CoCrFeNiCuTi<sub>0.3</sub> multicomponent high-entropy alloys. (Doctoral dissertation, Jiangsu University of Science and Technology).
- [10] Miao, Z., Zhu, F., & Liu, Q. (2020). Study on the microstructure and corrosion resistance of CoCrFeNiCuTi<sub>x</sub> high-entropy alloys. *Powder Metallurgy Technology*, 38(01), 10-17.
- [11] Shi, H. F., Li, D. C., Bai, Y., Zhang, Z. Q., Jin, X., & Li, Y. F. (2024). Influence of Ti content on the microstructure and properties of CoCrFeNiCuTi<sub>x</sub> high-entropy alloy coatings by argon arc cladding. *Journal of Materials Heat Treatment*, 45(03), 82-89.
- [12] Mendeleev, M. I., Underwood, T. L., & Ackland, G. J. (2016). Development of an interatomic potential for the simulation of defects, plasticity, and phase transformations in titanium. *The Journal of Chemical Physics*, 145(15), 154102.
- [13] Farkas, D., & Caro, A. (2018). Model interatomic potentials and lattice strain in a high-entropy alloy. *Journal of Materials Research*, 33(12), 1-15.
- [14] Halicioğlu, T., & Pound, G. M. (1975). Calculation of potential energy parameters from crystalline state properties. *physica status solidi (a)*, 30(2), 619-623.
- [15] Filippova, V. P., Kunavin, S. A., & Pugachev, M. S. (2015). Calculation of the parameters of the Lennard-Jones potential for pairs of identical atoms based on the properties of solid substances. *Inorganic Materials: Applied Research*, 6(1), 1-8.
- [16] Li, P., Roberts, B. P., Chakravorty, D. K., & Merz, K. M., Jr. (2015). Rational design of particle mesh Ewald compatible Lennard-Jones parameters for +2 metal cations in explicit solvent. *University of Florida*.
- [17] Brandt, E. G., & Lyubartsev, A. P. (2013). Systematic optimization of a force field for classical simulations of TiO<sub>2</sub>-water interfaces. *Journal of Chemical Theory and Computation*.